Available online at www.sciencedirect.com

ScienceDirect

Energy Procedia 158 (2019) 123–128

Energy Procedia

www.elsevier.com/locate/procedia

10th International Conference on Applied Energy, ICAE 2018, 22-25 August 2018, Hong Kong, China

A predicting model of PaTs' performance in off-design operating conditions

Mosè Rossi[a], Alessandra Nigro[a], Massimiliano Renzi[a,*]

[a]*Free University of Bozen-Bolzano, Faculty of Science and Technology, Piazza Università 1, Bolzano – 39100, Italy*

Abstract

The aim of this work is to propose a predicting model for evaluating Pump-as-Turbines' (PaTs) performance in off-design operating conditions. The predicting model has been derived from an elaboration of experimental test data available in literature on a set of several pumps operating in reverse mode. The performance prediction capability of the model has been compared with the results of the Computational Fluid Dynamics (CFD) analysis of a centrifugal pump running in turbine mode for several operating conditions. The comparison of the performance predicted by the model and the ones obtained with the numerical analysis has allowed to evaluate the effectiveness of the proposed model, highlighting its pros and cons and possible improvements. In general, it is possible to conclude that the proposed model is able to correctly assess the work and the efficiency of the studied PaT within errors in the range of few percentage points, especially for operating conditions not so far from the designed one.

Keywords: Centrifugal pump, Pump-as-Turbine, Best Efficiency Point, Performance prediction, Computational Fluid Dynamics

1. Introduction

The stringent emission targets imposed to reduce the environmental footprint of the human activities make the use of renewable energy sources no longer a choice but a crucial constraint [1]. Among the renewable energy sources, hydropower is the most spread worldwide. Nowadays, the technology available for large-scale hydropower is quite mature and the availability of unexploited geographical sites, where a large amount of water can be collected, is decreasing.

* Corresponding author.
E-mail address: Massimiliano.Renzi@unibz.it

1876-6102
10.1016/j.egypro.2019.01.056

Therefore, small-scale hydropower is becoming a valid alternative to the large-scale one. A promising technology and a suitable option for both energy recovery and distributed hydropower generation is the use of pumps running in reverse mode, which are also known as Pumps-as-Turbines (PaTs) [2]. Binama et al. [3] performed a detailed review of the PaT technology regarding the state-of-the-art and, along the same line, Jain et al. [4] carried out a review of different turbines and pumps, suitable to run in reverse mode, in several applications regarding micro-hydropower plants. In Water Distribution Networks (WDNs), PaTs can be also used for replacing Pressure Reducing Valves (PRVs) in order to have both pressure reduction and energy recovery [5]. Furthermore, besides WDNs, chemical industries have introduced PaTs for energy recovery, named High Power Recovery Turbines (HPRTs) [6]. Despite the great versatility and the spread use of PaTs, a correct definition of their performance is not straightforward since pump manufacturers do not provide experimental data in turbine mode. For this reason, some researchers [7-12] tried to develop different analytical and empirical formulations able to forecast flow rate and head of PaTs at the Best Efficiency Point (BEP) using the corresponding values in pump mode. Nevertheless, the prediction of PaTs performance in off-design operating conditions is still a challenge. The aim of this work is to characterize PaTs' performance far from the design point by means of a predicting model developed by the same authors of this work in [13]. The strength of the proposed model is that: i) it is based on a quite large experimental data-set; ii) it allows to evaluate in a straightforward way the main characteristics of a PaT in any operating conditions; iii) it consists of very simple correlations that do not require any specific design parameter that is rarely available to the final user. In order to assess and to evaluate the potential and the effectiveness of the proposed model, a Computational Fluid Dynamics (CFD) analysis of a centrifugal pump, running in turbine mode for several operating conditions, has been carried out. The results of both model and CFD analysis are presented and compared. Specifically, Section 2 is devoted to a brief description of the predicting model. In Section 3, the CFD set-up and the main numerical models used to perform the simulations are presented. The results obtained with the predicting model and with the CFD analysis are compared and discussed in Section 4. Finally, conclusions are reported in Section 5.

2. Predicting model

The proposed model predicts the behaviour of a pump used in reverse mode by means of very simple formulations derived from a statistical elaboration of experimental data. The experimental data-set collects the main performance parameters of 32 different hydraulic machines [12] operating at BEP and also in off-design operating conditions. These data referred to different PaTs operating ranges in terms of flow rate (0.008-0. 222 m^3/s), head (1.99-99.52 m), rotating speed (750-2445 rpm), impeller diameter (0.165-0.300 m), specific speed (0.17-2.39) and hydraulic efficiency (0.43-0.87). A non-dimensional analysis of the experimental data has been performed and the non-dimensional coefficients have been normalized with respect to their corresponding BEP's values. Finally, the normalized PaTs' characteristic and efficiency curves have been built interpolating the non-dimensional normalized data with polynomial functions, reported in Eq.s (1, 2), respectively.

$$\Psi/\Psi_{BEP} = 0.2394 \cdot (\Phi/\Phi_{BEP})^2 + 0.769 \cdot (\Phi/\Phi_{BEP}) \quad (1)$$

$$\eta/\eta_{BEP} = -1.9788 \cdot (\Phi/\Phi_{BEP})^6 + 9.0636 \cdot (\Phi/\Phi_{BEP})^5 - 13.148 \cdot (\Phi/\Phi_{BEP})^4 + 3.8527 \cdot (\Phi/\Phi_{BEP})^3 + 4.5614 \cdot (\Phi/\Phi_{BEP})^2 - 1.3769 \cdot (\Phi/\Phi_{BEP}). \quad (2)$$

The degrees of the polynomial interpolation functions have been chosen in order to preserve a good accordance between the values of the experimental data-set and the ones obtained with the predicting curves. Specifically, the R^2-values obtained for different degrees of the interpolation functions have been used to evaluate the agreement between the predicting model and the experimental values. The R^2-values that refer to Eq.s (1-2) are equal to 0.9171 and 0.7856, respectively. In Fig. 1, the experimental points and the interpolated characteristic and efficiency curves of Eq. 1 and 2 (Fig. 1.a and Fig. 1.b, respectively) are reported. It is interesting to notice that the curves in Fig. 1.a and Fig. 1.b have the same trend of the characteristic and efficiency curves of a generic hydraulic turbine. Finally, it is worth to notice that the hydraulic efficiency trend shows more spread-out data-set than the other graph: indeed, the R^2-value of the predicted efficiency curve is lower than the R^2-value that refers to the predicted characteristic curve.

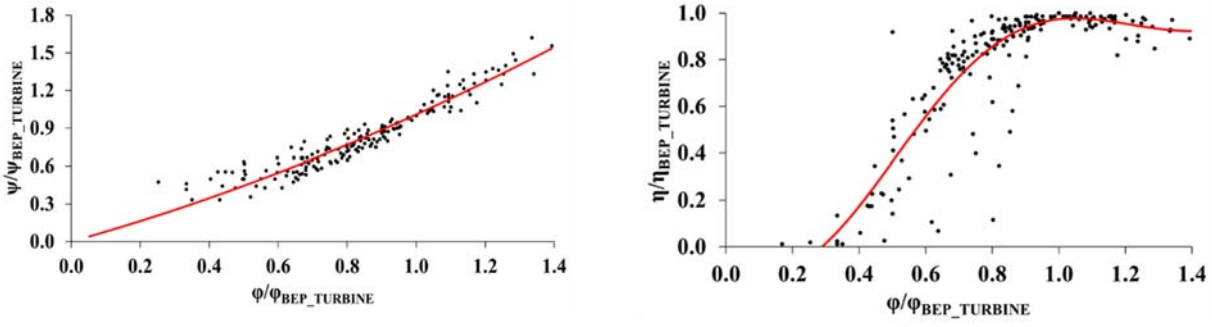

a) b)

Fig. 1. Non-dimensional normalized flow coefficient vs head coefficient (a), non-dimensional normalized flow coefficient vs efficiency (b).

3. CFD set-up

The flow solver, used to validate the predicting model by means of CFD analysis, is ANSYS-CFX®. The main PaT's characteristics in pump mode are listed in Table 1, whereas the computational fluid domain is shown in Fig. 2 where inlet and outlet boundaries are highlighted with arrows. Note that, in the computational domain, the length of the exit tube has been extended to about 5D beyond the real exit section of the PaT, being D the diameter of the exit section, in order to enable pressure conditions at the exit section to be fixed as reported in Table 2. The others adopted boundary conditions and their values are reported in the same table.

Table 1. PaT's characteristics

Pump type	Centrifugal
Impeller type	Shroudless
Number of blades	6
Rotating speed [rpm]	1450
Impeller diameter [m]	0.281
Flow rate BEP [m^3/s]	0.0775
Head BEP [m]	21.59
Specific speed (N_S)	0.76

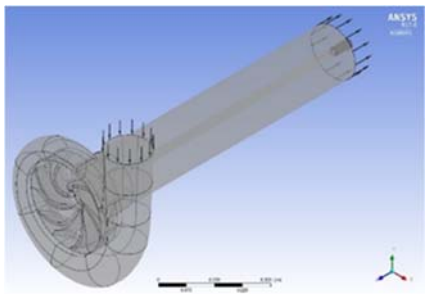

Fig. 2. Computational domain

Table 2. Boundary Conditions (BCs) used in CFD simulations

Type of boundary	Fluid dynamic parameters used as BCs	Turbulence parameters
Inflow	Volumetric Flow Rate normal to BC: [0.077-0.138] [m^3/s]	Intensity 5%
Outflow	Average Static Pressure with Radial Equilibrium: 1 [bar]	-
Wall	Heat flow=0 (adiabatic wall), Velocity=0 (no-slip condition)	-
Interface - Volute to Impeller	Conservative Interface Flux, Pitch Angles: 360 [degree]	Conservative Interface Flux
Interface - Impeller to Exit Tube	Conservative Interface Flux, Pitch Angles: 360 [degree]	Conservative Interface Flux

The interfaces named "Volute to Impeller" and "Impeller to Exit Tube" have been created to enable the Frozen Rotor Model (FRM). In fact, to take into account the relative rotation of the impeller with respect to the volute and the exit tube, the computational fluid domain has been broken-up into stationary (volute and exit tube) and moving (impeller) zones. The interaction between these zones have been model using the FRM. The FRM is a steady state method that uses rotating reference frame to reduce the computational effort [14]. Fig. 3.a shows a view of the volute and the exit-tube, Fig. 3.b shows the impeller computational grid and Table 3 reports the number and the type of elements used to discretize the computational domain. Grid independence has been ensured by successive mesh refinements.

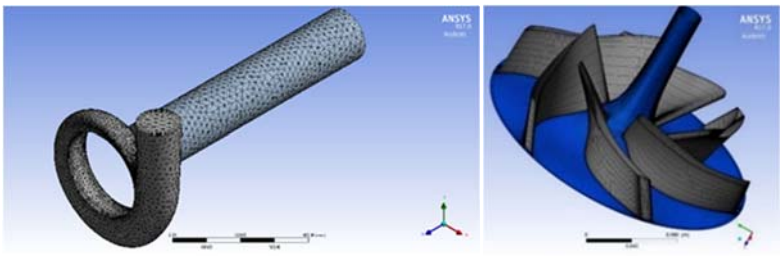

a) b)

Fig. 3. Computational grid of the volute together, with the exit tube (a), and of the impeller (b)

Table 3. Spatial discretization

Geometry	n° elements	Elements type
Volute	227,643	Tetrahedra & Wedges
Impeller	743,544	Hexahedra
Exit Tube	84,319	Tetrahedra, Wedges & Pyramids
Total	1,055,506	

Simulations are performed considering different mass flow rates in order to cover the overall operating range, whose ranges' variations. Specifically, the analysis is carried out by varying the mass flow rate by steps of 0.00775 m^3/s from a minimum of 0.077 m^3/s until a maximum of 0.138 m^3/s. Therefore, nine different operating points, BEP included (corresponding to 0.109 m^3/s), are simulated. The discretization of the governing equations is based on the Finite Volume Method (FVM). Convective and diffusive terms are discretized with High-Resolution schemes [15]. The pressure-velocity coupling uses a non-staggered grid layout similar to [16]. Reynolds Averaged Navier Stokes (RANS) equations augmented with the standard k-ω two-equation model are used for modelling the turbulence. The automatic wall function is employed for the near wall-treatment, which is a blending between viscous sublayer and log-law relation that allows a consistent y^+ insensitive mesh refinement. The convergence is checked by monitoring the Root Mean Square (RMS) residuals' variations between successive iterations and the calculation process is stopped when a very low percentage variation is reached. The normalized residuals drop, considering all the simulations, occurred between 10^{-5} and 10^{-10}.

4. Results and comments

In Table 4 and in Table 5, the results obtained by the CFD analysis and the predicting model are shown. In Table 4, the values of volumetric flow rate (Q) and head (H) are directly obtained by means of CFD analysis, while, in order to take in to account the mechanical friction losses, the efficiency (η) reported in Table 4 is equal to the one obtained with the numerical analysis times the mechanical efficiency, which is considered constant for every operating point and equal to 0.95. Finally, in the tables, mechanical power (P), specific speed (N_S), specific diameter (D_S) and non-dimensional values φ, ψ and Λ are calculated using the traditional formulations employed for studying hydraulic machines.

Table 4. PaT's performance parameters and their corresponding non-dimensional values obtained by CFD analysis

Q [m^3/s]	φ	H [m]	ψ	P [kW]	Λ	η	Ns	Ds
0.077	0.023	14.4	0.078	7.179	0.00118	0.66	1.03	3.49
0.085	0.025	16.0	0.086	9.606	0.00155	0.72	1.00	3.41
0.093	0.028	17.0	0.092	11.477	0.00191	0.74	1.00	3.31
0.101	0.030	18.7	0.101	14.452	0.00236	0.78	0.97	3.25
0.109	**0.032**	**20.8**	**0.112**	**17.571**	**0.00283**	**0.79**	**0.93**	**3.22**
0.115	0.034	22.7	0.122	20.231	0.00328	0.79	0.89	3.20
0.123	0.037	24.7	0.133	23.545	0.00389	0.79	0.87	3.16
0.130	0.039	26.9	0.145	27.101	0.00447	0.79	0.84	3.14
0.138	0.041	29.3	0.158	31.336	0.00512	0.79	0.81	3.11

Table 5. PaT's performance parameters and their corresponding non-dimensional values obtained by the predicting model

Q [m^3/s]	φ	H [m]	ψ	P [kW]	Λ	η	Ns	Ds
0.077	0.023	14.1	0.076	6.390	0.00105	0.60	1.04	3.47
0.085	0.025	15.6	0.084	8.585	0.00139	0.66	1.02	3.39
0.093	0.028	17.8	0.096	11.855	0.00196	0.73	0.96	3.35
0.101	0.030	19.3	0.104	14.533	0.00237	0.76	0.95	3.28
0.109	**0.032**	**21.0**	**0.113**	**17.290**	**0.00278**	**0.77**	**0.92**	**3.22**
0.115	0.034	22.6	0.122	19.632	0.00319	0.77	0.90	3.20
0.123	0.037	25.1	0.135	23.018	0.00380	0.76	0.86	3.17
0.130	0.039	26.9	0.145	25.729	0.00424	0.75	0.84	3.14
0.138	0.041	28.6	0.154	28.651	0.00467	0.74	0.82	3.10

The non-dimensional operating parameters ψ and η of the PaT were also calculated using the proposed Eq.s (1) and (2) as a function of φ; their values are reported in Table 5, together with the mechanical power output and the other non-dimensional parameters that are calculated similarly to the ones described in Table 4. In order to compare the reported results, Fig. 4 shows the trend of ψ (Fig. 4.a), η (Fig. 4.b) and Λ (Fig. 4.c) as functions of φ, obtained by the CFD analysis (red circle symbols) and by the model (blue diamond symbols). The results obtained using the predicting model are in accordance with the ones of the numerical analysis.

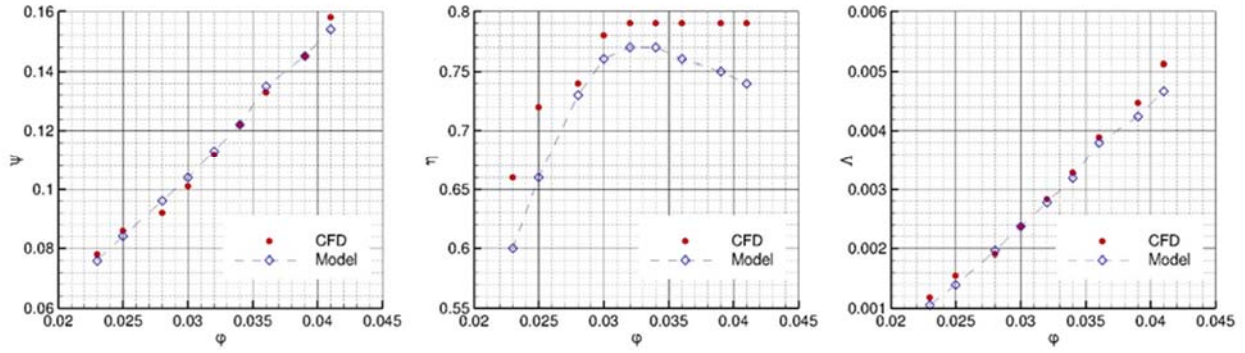

a) b) c)

Fig. 4. Comparison between CFD and predicting model as a function of the flow coefficient: a) head coefficient; (b) mechanical efficiency; (c) mechanical power coefficient.

A quantitative analysis is reported in Table 6 where the percentage relative differences between predicted and simulated values are reported. The percentage relative difference of a generic variable a has been defined as:

$$\Delta\, a\ (\%) = (a_{CFD} - a_{model})/a_{model}. \quad (3)$$

The table shows that the BEP value, reported in bold, is well predicted with a maximum percentage relative difference of 2.6% for the efficiency. Furthermore, there is a general good agreement between CFD and predicting model values, even in off-design operating conditions near the BEP. Nevertheless, when the PaT is operating with significantly higher or lower flow rates, the percentage relative differences of the non-dimensional parameters tend to increase. The increase of uncertainty when the predicting model is used in these extreme operating conditions is mainly due to the nature of the experimental data-set from which the model has been derived. In fact, Fig. 1.b evidences that the experimental values are much more dispersed when dealing with off-design operating conditions than the ones close to the PaTs BEP. Furthermore, far from the BEP, the number of experimental data is lower.

Table 6. Percentage relative differences between CFD and predicting model

φ	φ/φ_{BEP}	Δ ψ (%)	Δ η (%)	Δ Λ (%)	Δ Ns (%)	Δ Ds (%)
0.023	0.719	2.6	10.0	12.4	-1.0	0.6
0.025	0.781	2.4	9.1	11.8	-2.0	0.6
0.028	0.875	-4.2	1.4	-2.7	4.2	-1.2
0.030	0.937	-2.9	2.6	-0.5	2.1	-0.9
0.032	**1.000**	**-0.9**	**2.6**	**1.6**	**1.1**	**0.0**
0.034	1.062	0.0	2.6	2.7	-1.1	0.0
0.037	1.156	-1.5	3.9	2.5	1.2	-0.4
0.039	1.219	0.0	5.3	5.4	0.0	0.0
0.041	1.281	2.6	6.8	9.6	-1.2	0.5

5. Conclusions

In this work, the performance prediction of a PaT operating at design and in off-design operating conditions has been carried out using a CFD analysis and a predicting model derived from an experimental data-set. The comparison between the values obtained by the CFD analysis and by the predicting model shows a very good accordance of the two methodologies on forecasting the PaTs' performance in off-design operating conditions not so far from the BEP, while a slight mismatch is shown when operating far from it. Future work will be devoted to improve the proposed model by increasing the experimental data derived by PaTs' tests, especially for extremely off-design operating conditions, and to carry on further CFD analyses on different designs of hydraulic machines.

References

[1] Z. Said, A.A. Alshehhi, A. Mehmood. Predictions of UAE's renewable energy mix in 2030, Renewable Energy, Year 2018, Vol. 118, Pages 779-789.
[2] Z. Zuo, H. Fan, S. Liu, Y. Wu. S-shaped characteristics on the performance curves of pump-turbines in turbine mode – A review, Renewable and Sustainable Energy Reviews, Year 2016, Vol. 60, Pages 836-851.
[3] M. Binama, W-T. Su, X-B. Li, F-C. Li, X-Z. Wei, S. An. Investigation on pump as turbine (PAT) technical aspects for micro hydropower schemes: A state-of-the-art review, Renewable and Sustainable Energy Reviews, Year 2017, Vol. 79, Pages 148-179.
[4] S.V. Jain, R.N. Patel. Investigations on pump running in turbine mode: A review of the state-of-the-art, Renewable and Sustainable Energy Reviews, Year 2014, Vol. 30, Pages 841-868.
[5] M. Rossi, M. Righetti, M. Renzi. Pump-as-turbine for Energy Recovery Applications: The Case Study of An Aqueduct, Energy Procedia, Year 2016, Vol. 101, Pages 1207–1214.
[6] R. Singh, S.V. Cabibbo. Hydraulic turbine energy recovery - R.O. System, Desalination, Year 1980, Vol. 32, Pages 281–296.
[7] Williams A., The Turbine Performance of Centrifugal Pumps: A Comparison of Prediction Methods, Journal of Power and Energy, 1994, vol. 208, p. 59-66.
[8] Stepanoff A., Centrifugal and Axial Flow Pumps, Design and Applications, John Wiley and Sons, Inc. New York, USA, 1997.
[9] Krivchenko G., Hydraulic Machines: Turbines and Pumps, Lewis, Boca Raton, Fla., USA, 1994.
[10] Sharma K., Small Hydroelectric Project-Use of Centrifugal Pumps as Turbines. Technical Report, Kirloskar, Electric Co. Bangalore, India, 1985.
[11] McClaskey B. et al., Can You Justify Hydraulic Turbines?. Hydrocarbon Processing, 1976, vol. 55, p. 163-169.
[12] M. Rossi, M. Renzi. A general methodology for performance prediction of pumps-as-turbines using Artificial Neural Networks, Renewable Energy, Year 2018, Vol. 128 Part A, Pages 265-274.
[13] M. Rossi, M. Renzi. Analytical Prediction Models for Evaluating Pumps-As-Turbines (PaTs) Performance, Energy Procedia, Year 2017, Vol. 118, Pages 238–242.
[14] ANSYS-CFX Solver Modeling Guide Release 18.2 - © ANSYS, Inc.
[15] T.J. Barth, D.C. Jesperson. The Design and Application of Upwind Schemes on Unstructured Meshes, AIAA, Paper 89-0366, 1989.
[16] S. Majumdar. Role of Underrelaxation in Momentum Interpolation for Calculation of Flow with Nonstaggered Grids, Numerical Heat Transfer, Year 1988, Vol. 13, Pages 125–132.